engineering proceedings

Proceeding Paper

Preliminary Evaluation of *Arenga pinnata* Nutshell-Derived Carbon in a Membrane-Assisted Electrochemical Cell for Sodium Chloride Treatment †

Jewel Rose B. Barbon [1], Andrei B. Matias [1], Abigail D. Monis [1], John Paul M. Parani [1], Paul JenRae Q. Samson [1], Coleen Moira O. Sarmiento [1], Jerry G. Olay [1,2], Rugi Vicente C. Rubi [1,2] and Rich Jhon Paul D. Latiza [1,2,*]

[1] Chemical Engineering Department, College of Engineering, Adamson University, 900 San Marcelino St., Ermita, Manila 1000, Philippines; barbon.jewel.rose@adamson.edu.ph (J.R.B.B.); andrei.matias@adamson.edu.ph (A.B.M.); abigail.monis@adamson.edu.ph (A.D.M.); john.paul.parani@adamson.edu.ph (J.P.M.P.); pauljenraesamsonz@gmail.com (P.J.Q.S.); coleen.moira.sarmiento@adamson.edu.ph (C.M.O.S.); jerry.olay@adamson.edu.ph (J.G.O.); rugi.vicente.rubi@adamson.edu.ph (R.V.C.R.)

[2] Laboratory of Biomass, Energy and Nanotechnology (ALBEN), Adamson University, 900 San Marcelino St., Ermita, Manila 1000, Philippines

* Correspondence: rich.jhon.paul.latiza@adamson.edu.ph

† Presented at the 3rd International Online Conference on Energies (IOCEN 2026), 12–15 May 2026; Available online: https://sciforum.net/event/IOCEN2026.

Abstract

Arenga pinnata nutshell-derived carbon was prepared by heat treatment and KOH treatment, incorporated into a cathode, and evaluated in a membrane-assisted electrochemical cell. Available SEM–EDX observations describe the prepared material but do not establish its pore structure or potassium speciation. Across the tested temperature and flow conditions, the highest mean decrease in effluent sodium concentration was 71.27 ± 0.73% at 15 °C and 5 mL/min. Incomplete electrochemical records and the absence of matched control electrodes prevent assignment of a battery-type mechanism or a performance advantage. These results provide preliminary cell-level observations and identify the validation needed for further assessment.

Keywords: *Arenga pinnata*; biomass-derived carbon; membrane-assisted electrochemical cell; sodium removal; SEM–EDX; preliminary evaluation

1. Introduction

Water-quality challenges in the Philippines motivate investigation of additional treatment options [1]. Water and wastewater treatment technologies must also be considered in relation to resource recovery and energy requirements [2]. Electrochemical treatment can combine electrodes and ion-exchange membranes, but measured changes in solution composition must be distinguished from evidence for a particular electrode-storage mechanism.

Battery electrode deionization (BDI) has been demonstrated using electrodes with established reversible ion-storage behavior, including paired copper hexacyanoferrate electrodes [3]. Battery deionization has also been investigated for ammonium and phosphate recovery in a background electrolyte [4]. The presence of ion-exchange membranes and an applied voltage alone does not establish that an experimental cell operates by the same mechanism. The present device is therefore described as a membrane-assisted electrochemical cell. Its aluminum anode and nutshell-derived carbon cathode are identified by their

Check for updates

Academic Editor: Said Al-Hallaj

Published: 28 October 2026

Copyright: © 2026 by the authors. Licensee MDPI, Basel, Switzerland. This article is an open access article distributed under the terms and conditions of the Creative Commons Attribution (CC BY) license.

roles in the reported configuration; battery-type storage and the relative contributions of membrane transport and electrode reactions remain unresolved.

Biomass-derived carbons have been investigated as electrode materials [5]. Nutshell conversion has been studied for cashew, argan, and pecan residues, using different preparation routes and evaluating different products or adsorption applications [6–8]. Agricultural-waste biochar composites have also been reviewed for supercapacitors [9]. These studies provide background for precursor selection; their performance cannot be transferred to the present cell. Here, Kaong (*Arenga pinnata*) nutshells were examined as a locally sourced carbon precursor. The study reports the available material observations and the changes in effluent sodium concentration across selected operating conditions. It does not establish a new cell principle, an optimized synthesis route, or superiority over conventional cathodes. The use of a biomass precursor is a material-selection rationale; cost, environmental benefit, and electrochemical performance require separate comparison.

2. Materials and Methods

2.1. Materials and Pretreatment

Kaong (*Arenga pinnata*) nutshells were collected in Indang, Cavite, and submitted for taxonomic identification to the Department of Agriculture Bureau of Plant Industries (BPI, Manila, Philippines). The shells were washed with distilled water and oven-dried at 105 °C for 5 h. Oven-drying studies on other biological materials show that moisture determinations depend on the drying conditions and sample matrix [10]; they do not independently validate this pretreatment for Kaong shells. KOH, HCl, NaCl, polyvinylidene fluoride (PVDF), and N-methyl-2-pyrrolidone were used in material preparation or testing. Commercial cation-exchange and anion-exchange membranes (CEM and AEM) were obtained from the Fuel Cell Store (Bryan, TX, USA). Separate compositional or structural characterization of the as-received shells, reagents, membranes, and current collectors is not reported.

2.2. Preparation of Nutshell-Derived Carbon

The dried shells were heat-treated in a muffle furnace (M110, Heraeus, Hanau, Germany) at the Department of Science and Technology–Industrial Technology Development Institute (DOST-ITDI, Taguig, Philippines) at 500 °C for 3 h. The resulting material was pulverized and passed through a 100-mesh sieve. The recorded KOH treatment used a KOH-to-char ratio of 2:1 by mass, followed by grinding, treatment with an HCl–water solution, and drying at 100 °C. Furnace atmosphere, acid concentration, washing endpoint, and any separate post-impregnation heat-treatment step are not sufficiently documented in the available record. The product is referred to here as KOH-treated nutshell-derived carbon; increased porosity and complete removal of residual potassium are not assumed. Studies of KOH activation and impregnation ratios in other carbon precursors illustrate why treatment conditions require material-specific evaluation [11,12]; those studies are not validation of the present preparation route.

2.3. Electrode Preparation and Available Material Characterization

The treated carbon was mixed with a 10% PVDF binder solution in N-methyl-2-pyrrolidone, applied to both faces of stainless-steel mesh, and pressed. The assembly was immersed in deionized water for 15 min and air-dried for 8 h. PVDF has been studied as an electrode binder [13], but the present coating adhesion and binder contribution were not independently quantified. The available SEM–EDX report from NASAT Labs (Muntinlupa, Philippines) identifies the submitted sample as “Biochar Koang Nuts”, mounted on an aluminum stub and examined using a Hitachi SU8600 scanning electron microscope (Hi-

tachi High-Tech Corp., Tokyo, Japan) and an Oxford Ultim Extreme EDX system (Oxford Instruments, High Wycombe, UK). These observations characterize the submitted prepared material, rather than a verified before-and-after series of the raw shells, finished composite electrode, and used electrode. SEM–EDX provides morphological and elemental information, but does not independently establish bulk composition, pore-size distribution, or chemical speciation [14].

2.4. Cell Configuration and Sodium-Concentration Measurements

The cell contained an aluminum anode, a carbon-coated stainless-steel-mesh cathode. The components were held between acrylic end plates. The source description gives nominal electrode dimensions of 4 × 4 inches, with liquid flowing along the electrode gaps without a fabric spacer. Feed temperatures of 15, 25, and 30 °C and inlet flow rates of 5, 15, and 25 mL/min were investigated. The recorded electrical settings were 10 A/m^2, ±0.6 V, and approximately 3 min per cycle; individual electrode potentials were not established. These settings do not exclude electrode side reactions, aluminum dissolution, or water electrolysis.

The preparation record describes dissolving 1 g NaCl in 1 L of water. However, the AAS feed certificate reports sodium at 964 mg/L, which is inconsistent with that nominal preparation. The preparation and dilution records therefore require reconciliation. The measured feed and effluent sodium concentrations are used here, without treating the nominal recipe as a verified salinity. Flame atomic absorption spectroscopy (AAS; Mach Union Laboratory, Inc., Pasig, Philippines) measured sodium; no corresponding chloride balance is available. The relative sodium concentration reduction was calculated as $100 \times (C_{in} - C_{out})/C_{in}$, using the same sodium concentration basis for both streams.

2.5. Scope of Electrochemical and Data Analysis

Exploratory cyclic voltammetry (CV) and electrochemical impedance spectroscopy (EIS) measurements were undertaken at the Department of Mining, Metallurgical, and Materials Engineering, University of the Philippines Diliman (Quezon City, Philippines). The CV descriptions refer to 0.3 M NaCl and scan rates of 5 and 10 mV/s, but the run-to-scan-rate assignment, potential reference, and scan windows are not consistently documented. The EIS record does not provide a reconciled frequency-labeled dataset, perturbation amplitude, or DC bias sufficient for reproducible fitting. Accordingly, these measurements are not used to extract kinetic parameters or establish a sodium-storage mechanism. Sodium concentration results are summarized descriptively as means and sample standard deviations across three reported runs per condition using Microsoft Excel (Microsoft 365, Microsoft Corporation, Redmond, WA, USA); the variability is not an estimate of reproducibility between independently fabricated electrodes.

3. Results and Discussion

3.1. Observations on the Prepared Material

Figure 1 reproduces the SEM field from the original laboratory report, including its scale bar. Rough, irregular particles and smaller approximately rounded features are visible. This observation does not quantify microporosity, mesoporosity, accessible surface area, wettability, conductivity, or structural stability. Those properties cannot be inferred solely from the apparent surface texture. Accessible surface area and pore-size distribution can affect carbon-electrode capacitance [15], which supports the need to measure these properties directly before relating morphology to electrochemical behavior.

https://doi.org/10.3390/engproc2026147024

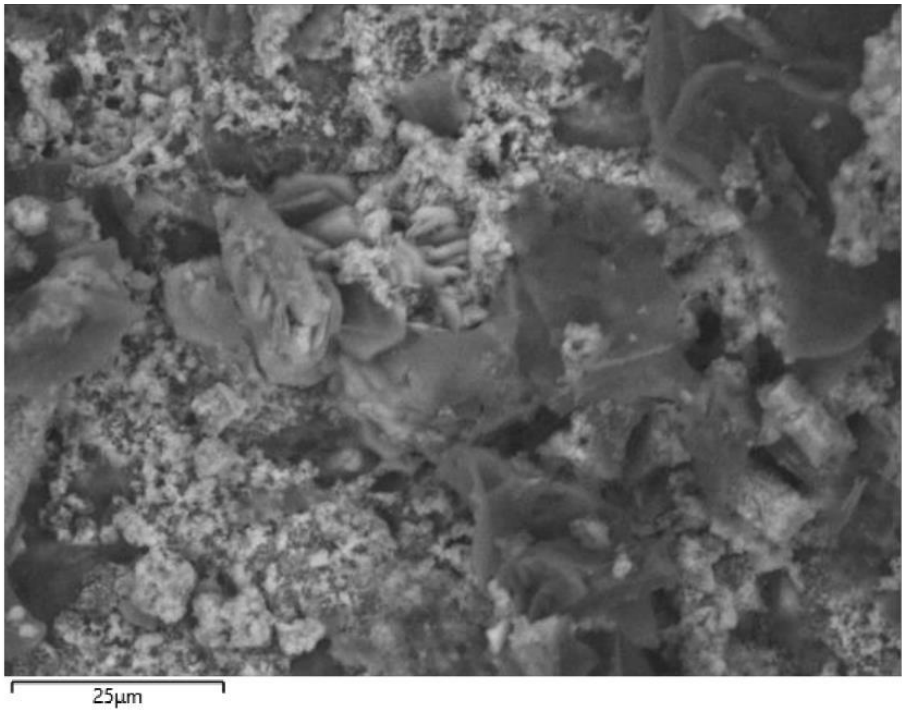


Figure 1. SEM image of the submitted nutshell-derived material from the original NASAT Labs report. The original 25 µm scale bar is retained; no particle-size distribution is inferred.

The original map-sum EDX spectrum (Figure 2) reports O 38.1, K 37.8, Ca 7.7, Cl 7.6, Si 4.4, Al 2.9, Mg 0.7, P 0.3, Na 0.3, and S 0.1 wt%. Although the spectrum contains a carbon signal, the laboratory quantification table does not give a carbon weight fraction. The percentages describe the reported map-sum analysis and must not be treated as a measured bulk carbon composition. The aluminum mounting stub may also contribute to the Al signal.

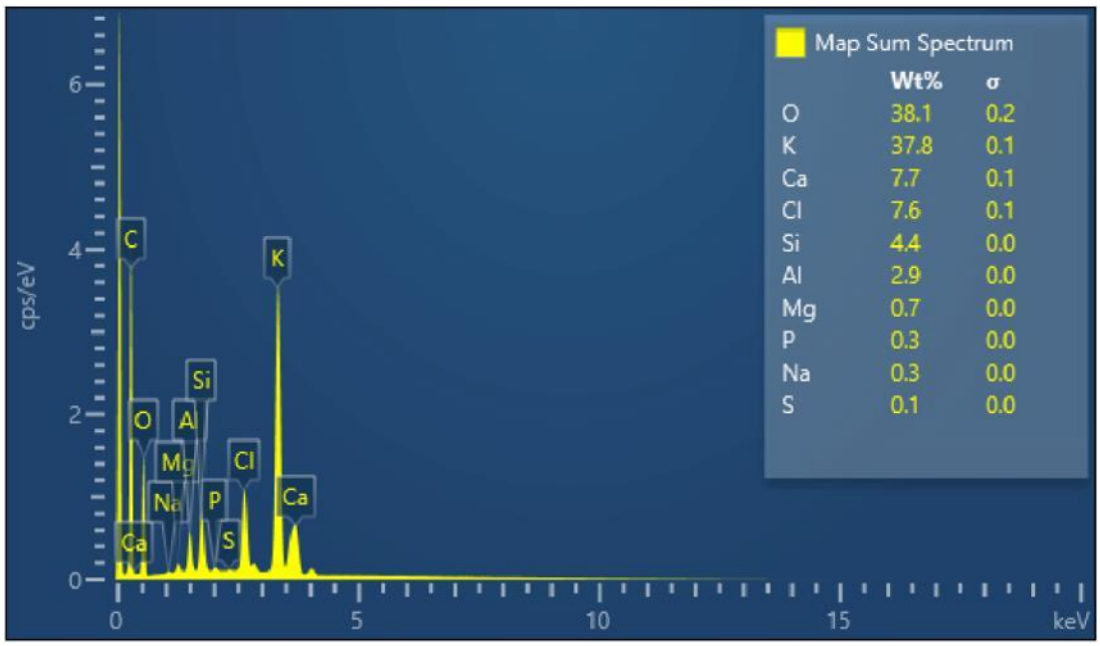


Figure 2. Original NASAT Labs map-sum EDX spectrum and quantification table for the submitted material. The table reports O at 38.1 wt% and K at 37.8 wt%; it does not report a carbon weight fraction.

https://doi.org/10.3390/engproc2026147024

The substantial potassium signal may reflect retained material from KOH treatment, but its chemical form and its effect on operation are undetermined. Elemental percentages alone do not identify a potassium counterion or distinguish hydroxides, oxides, carbonates, and other phases. Direct characterization of the as-received materials and the finished and used electrodes, including appropriate phase, surface, porosity, and leaching measurements, remains necessary before connecting material structure or composition to performance.

3.2. Limits of the Electrochemical Evidence

The available CV curves cannot support a controlled comparison between 5 and 10 mV/s because the run identities and potential scales are not consistently documented. Consequently, the records do not establish reversible Na^+ intercalation or scan-rate-dependent kinetics. Repeat, traceable scans with a defined electrode configuration and potential reference, together with blank and reference-material controls, are needed to distinguish carbon charging from other electrochemical processes. CV interpretation requires documented cell and scan parameters [16,17], while evaluation of reversibility requires attention to peak positions and their behavior with scan rate [18].

An apparent impedance arc does not uniquely identify an equivalent circuit, particularly for an assembled cell containing electrodes, membranes, and solution compartments [19–21]. The available records are insufficient for a validated quantitative interpretation. No equivalent-circuit fit, resistance parameters, fitting residuals, goodness-of-fit statistics, or parameter uncertainties are reported. The data do not establish reduced resistance, enhanced charge transfer, or the presence or absence of diffusion control. A repeat dataset with frequency labels and documented acquisition conditions, followed by validity checks and comparison of physically justified models, is required.

3.3. Sodium-Concentration Changes Across Tested Conditions

Figure 3 shows the reported component arrangement. The schematic describes the intended cell configuration; it is not evidence of intercalation, a resolved reaction pathway, or an absence of electrolysis. Table 1 summarizes the measured feed–effluent sodium concentration changes. The feed value used in these calculations is 964 mg Na/L, as reported by the laboratory certificate.

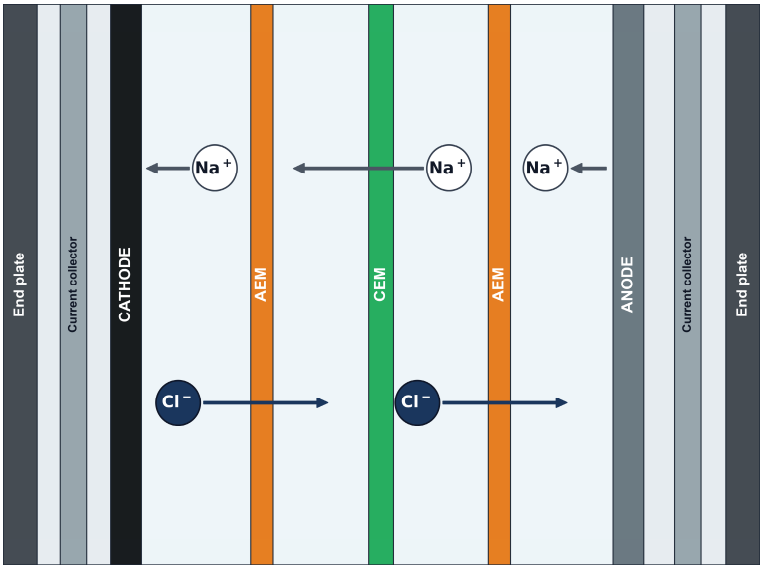


Figure 3. Reported component arrangement with a carbon-coated cathode, aluminum anode, and AEM–CEM–AEM stack. Arrows are schematic indications of ion movement and do not establish ion storage or electrode reactions.

Table 1. Effluent sodium concentration and relative concentration reduction across the tested conditions.

Temperature (°C)	Flow Rate (mL/min)	Effluent Na (mg/L)	Na Reduction (%)
15	5	277.0 ± 7.0	71.27 ± 0.73
15	15	345.0 ± 6.0	64.21 ± 0.62
15	25	479.0 ± 8.0	50.31 ± 0.83
25	5	362.3 ± 17.0	62.41 ± 1.76
25	15	496.7 ± 8.6	48.48 ± 0.89
25	25	596.7 ± 19.7	38.11 ± 2.04
30	5	490.3 ± 6.0	49.14 ± 0.63
30	15	577.7 ± 7.4	40.08 ± 0.76
30	25	697.7 ± 5.7	27.63 ± 0.59

Values are mean ± sample standard deviation for three reported runs per condition ($n = 3$). Percentages were recalculated from the recorded sodium concentrations using C_{in} = 964 mg Na/L. Between-electrode reproducibility and a complete sodium mass balance were not determined.

Within each tested temperature, increasing flow rate was associated with a smaller reduction in sodium concentration. At 15 °C, the mean reduction decreased from 71.27% at 5 mL/min to 50.31% at 25 mL/min. At 5 mL/min, the corresponding values decreased from 71.27% at 15 °C to 49.14% at 30 °C. Longer liquid residence at lower flow is a possible explanation, but residence time and the separate transport processes were not measured. The temperature trend is reported empirically; it does not demonstrate changes in fouling, ion intercalation, or intrinsic electrode kinetics. Flow-dependent separation has been examined in redox-flow desalination and microfluidic dialysis [22,23]. Their different geometries and transport processes prevent direct quantitative comparison with the present cell.

The highest mean reduction occurred at the lowest tested temperature and flow rate. This identifies the best of the reported conditions, rather than a validated optimum outside the tested range. The present analysis does not report a mass-normalized adsorption capacity because the treated-volume and electrode-mass basis of the earlier calculation is not adequately reconciled. A decline in effluent sodium concentration alone cannot establish sodium storage in the cathode, total NaCl removal, regeneration, or overall salt balance.

No matched comparison with a commercial carbon cathode, an uncoated current collector, or an open-circuit cell is available. It is therefore not possible to determine whether the nutshell-derived cathode improves performance over existing materials or to separate its contribution from membrane transport and other cell processes. Energy consumption, aluminum release, pH, gas formation, chloride balance, and cycling stability were not established. These limitations preclude claims of low-energy operation, water-treatment safety, electrode superiority, or practical readiness. Operational-mode comparisons in flow-electrode capacitive deionization [24] further illustrate the need to specify the cell configuration when comparing results. Broader desalination assessments also address energy supply [25] and concentrate impacts [26]; neither was quantified here.

4. Conclusions

Kaong nutshell-derived material was prepared, incorporated into a cathode, and used in a membrane-assisted electrochemical cell. The available SEM–EDX observations describe a heterogeneous, potassium- and oxygen-rich analyzed region, without establishing the bulk carbon fraction, potassium species, or pore structure. The largest mean reduction in effluent sodium concentration among the tested conditions was 71.27 ± 0.73% at 15 °C and

5 mL/min. This result is a preliminary cell-level observation. It does not establish a BDI mechanism or an advantage over conventional cathodes. Reconciled operating and analytical records, direct material characterization, validated electrochemical measurements, matched controls, and ion and charge balances are needed before making mechanistic or comparative conclusions.

Author Contributions: J.R.B.B., A.B.M., A.D.M., J.P.M.P., P.J.Q.S. and C.M.O.S.: conceptualization, data curation, formal analysis, investigation, methodology, validation, visualization, writing—original draft. R.V.C.R. and J.G.O.: conceptualization, data curation, project administration, supervision, validation, writing—review and editing. R.J.P.D.L.: visualization, writing—review and editing. All authors have read and agreed to the published version of the manuscript.

Funding: This research received no external funding.

Institutional Review Board Statement: Not applicable.

Informed Consent Statement: Not applicable.

Data Availability Statement: The authors declare that the data supporting the findings of this study are available within the paper. Should any raw data files be needed in another format, they are available from the corresponding author upon reasonable request.

Conflicts of Interest: The authors declare no conflicts of interest.

References

1. Tuddao, V.B., Jr. Progress of Water Environment Governance in the Philippines. In Proceedings of the 14th WEPA Annual Meeting, Tokyo, Japan, 23–24 January 2019.
2. Tetteh, E.K.; Rathilal, S.; Chetty, M.; Armah, E.K.; Asante-Sackey, D. Treatment of Water and Wastewater for Reuse and Energy Generation—Emerging Technologies. In *Water and Wastewater Treatment*; Eyvaz, M., Ed.; IntechOpen: London, UK, 2019; pp. 1–21. [CrossRef]
3. Kim, T.; Gorski, C.A.; Logan, B.E. Low Energy Desalination Using Battery Electrode Deionization. *Environ. Sci. Technol. Lett.* **2017**, *4*, 444–449. [CrossRef]
4. Son, M.; Aronson, B.L.; Yang, W.; Gorski, C.A.; Logan, B.E. Recovery of ammonium and phosphate using battery deionization in a background electrolyte. *Environ. Sci. Water Res. Technol.* **2020**, *6*, 1688–1696. [CrossRef]
5. Chen, H.; Liu, D.; Shen, Z.; Bao, B.; Zhao, S.; Wu, L. Functional Biomass Carbons with Hierarchical Porous Structure for Supercapacitor Electrode Materials. *Electrochim. Acta* **2015**, *180*, 241–251. [CrossRef]
6. Sengar, S.H.; Mohod, A.G.; Khandetod, Y.P. Performance Evaluation of Kiln for Cashew Nut Shell Carbonization and Liquid. *Int. J. Energy Eng.* **2012**, *2*, 78–85. [CrossRef]
7. Zbair, M.; Bottlinger, M.; Ainassaari, K.; Ojala, S.; Stein, O.; Keiski, R.L.; Bensitel, M.; Brahmi, R. Hydrothermal Carbonization of Argan Nut Shell: Functional Mesoporous Carbon with Excellent Performance in the Adsorption of Bisphenol A and Diuron. *Waste Biomass Valorization* **2020**, *11*, 1565–1584. [CrossRef]
8. Torres-Pérez, J.; Soria-Serna, L.A.; Solache-Ríos, M.; McKay, G. One Step Carbonization/Activation Process for Carbonaceous Material Preparation from Pecan Shells for Tartrazine Removal and Regeneration after Saturation. *Adsorp. Sci. Technol.* **2015**, *33*, 895–913. [CrossRef]
9. Khedulkar, A.P.; Dang, V.D.; Thamilselvan, A.; Doong, R.; Pandit, B. Sustainable high-energy supercapacitors: Metal oxide-agricultural waste biochar composites paving the way for a greener future. *J. Energy Storage* **2024**, *77*, 109723. [CrossRef]
10. Ahn, J.Y.; Kil, D.Y.; Kong, C.; Kim, B.G. Comparison of Oven-drying Methods for Determination of Moisture Content in Feed Ingredients. *Asian-Australas. J. Anim. Sci.* **2014**, *27*, 1615–1622. [CrossRef]
11. Wazir, A.H.; Haq, I.u.; Manan, A.; Khan, A. Preparation and characterization of activated carbon from coal by chemical activation with KOH. *Int. J. Coal Prep. Util.* **2022**, *42*, 1477–1488. [CrossRef]
12. Mutegoa, E.; Onoka, I.; Hilonga, A. Preparation of Activated Carbon with Desired Properties Through Optimization of Impregnating Agent. *Res. J. Eng. Appl. Sci.* **2014**, *3*, 327–331.
13. Zhong, X.; Han, J.; Chen, L.; Liu, W.; Jiao, F.; Zhu, H.; Qin, W. Binding mechanisms of PVDF in lithium ion batteries. *Appl. Surf. Sci.* **2021**, *553*, 149564. [CrossRef]
14. Ali, A.; Zhang, N.; Santos, R.M. Mineral characterization using Scanning Electron Microscopy (SEM): A review of the fundamentals, advancements, and research directions. *Appl. Sci.* **2023**, *13*, 12600. [CrossRef]

15. Zhang, L.; Yang, X.; Fan, Z.; Long, G.; Zhang, T.; Leng, K.; Zhang, Y.; Huang, Y.; Ma, Y.; Zhang, M.; et al. Controlling the Effective Surface Area and Pore Size Distribution of sp2 Carbon Materials and Their Impact on the Capacitance Performance of These Materials. *J. Am. Chem. Soc.* **2013**, *135*, 5921–5929. [CrossRef]
16. JoVE. Cyclic Voltammetry (CV): Measuring Redox Potentials and Currents. Available online: https://www.jove.com/v/5502/cyclic-voltammetry-cv-measuring-redox-potentials-and-currents (accessed on 3 September 2026).
17. Ossila. Cyclic Voltammetry Basic Principles, Theory & Setup. Available online: https://www.ossila.com/pages/cyclic-voltammetry (accessed on 3 September 2026).
18. Graham, D. Evaluating Electrochemical Reversibility. Standard Operating Procedures for Cyclic Voltammetry. Available online: https://sop4cv.com/chapters/EvaluatingElectrochemicalReversibility.html (accessed on 3 September 2026).
19. Lazanas, A.C.; Prodromidis, M.I. Electrochemical Impedance Spectroscopy—A tutorial. *ACS Meas. Sci. Au* **2023**, *3*, 162–193. Correction in *ACS Meas. Sci. Au* **2025**, *5*, 156. [CrossRef]
20. Magar, H.S.; Hassan, R.Y.A.; Mulchandani, A. Electrochemical impedance spectroscopy (EIS): Principles, construction, and biosensing applications. *Sensors* **2021**, *21*, 6578. [CrossRef]
21. Randviir, E.P.; Banks, C.E. Electrochemical impedance spectroscopy: An overview of bioanalytical applications. *Anal. Methods* **2013**, *5*, 1098–1115. [CrossRef]
22. Maclean, S.A.; Raza, S.A.; Wang, H.; Igbomezie, C.O.; Liu, J.; Makowski, N.; Ma, Y.; Shen, Y.; Röhr, J.A.; Weng, G.; et al. Investigation of flow rate in symmetric four-channel redox flow desalination system. *Cell Rep. Phys. Sci.* **2024**, *5*, 101761. [CrossRef]
23. Kalikavunkal, P.C.; Green, N.G.; de Planque, M.R.R. Tuning of salt separation efficiency by flow rate control in microfluidic dynamic dialysis. *Microfluid. Nanofluidics* **2019**, *23*, 111. [CrossRef]
24. Luo, K.; Niu, Q.; Zhu, Y.; Song, B.; Zeng, G.; Tang, W.; Ye, S.; Zhang, J.; Duan, M.; Xing, W. Desalination behavior and performance of flow-electrode capacitive deionization under various operational modes. *Chem. Eng. J.* **2020**, *389*, 124051. [CrossRef]
25. Sayed, E.T.; Olabi, A.G.; Elsaid, K.; Al Radi, M.; Alqadi, R.; Abdelkareem, M.A. Recent progress in renewable energy based-desalination in the Middle East and North Africa MENA region. *J. Adv. Res.* **2023**, *48*, 125–156. [CrossRef]
26. Omerspahic, M.; Al-Jabri, H.; Siddiqui, S.A.; Saadaoui, I. Characteristics of desalination brine and its impacts on marine chemistry and health, with emphasis on the Persian/Arabian Gulf: A review. *Front. Mar. Sci.* **2022**, *9*, 845113. [CrossRef]

Disclaimer/Publisher's Note: The statements, opinions and data contained in all publications are solely those of the individual author(s) and contributor(s) and not of MDPI and/or the editor(s). MDPI and/or the editor(s) disclaim responsibility for any injury to people or property resulting from any ideas, methods, instructions or products referred to in the content.